minerals

MDPI

Article

Recovery of Metals from Waste Lithium Ion Battery Leachates Using Biogenic Hydrogen Sulfide

Giles Calvert [1,2], Anna H. Kaksonen [1,2], Ka Yu Cheng [1,3], Jonovan Van Yken [1,4], Barbara Chang [2] and Naomi J. Boxall [1,*]

1 CSIRO Land and Water, 147 Underwood Avenue, Floreat, WA 6014, Australia; gilescalvert@gmail.com (G.C.); anna.kaksonen@csiro.au (A.H.K.); kayu.cheng@csiro.au (K.Y.C.); jonovan.vanyken@csiro.au (J.V.Y.)
2 School of Biomedical Sciences, The University of Western Australia, 35 Stirling Highway, Nedlands, WA 6009, Australia; barbara.chang@uwa.edu.au
3 School of Engineering and Information Technology, Murdoch University, Perth, WA 6150, Australia
4 School of Veterinary and Life Sciences, Murdoch University, Perth, WA 6150, Australia
* Correspondence: naomi.boxall@csiro.au; Tel.: +61-8-9333-6260

Received: 14 August 2019; Accepted: 14 September 2019; Published: 17 September 2019

Abstract: Lithium ion battery (LIB) waste is increasing globally and contains an abundance of valuable metals that can be recovered for re-use. This study aimed to evaluate the recovery of metals from LIB waste leachate using hydrogen sulfide generated by a consortium of sulfate-reducing bacteria (SRB) in a lactate-fed fluidised bed reactor (FBR). The microbial community analysis showed *Desulfovibrio* as the most abundant genus in a dynamic and diverse bioreactor consortium. During periods of biogenic hydrogen sulfide production, the average dissolved sulfide concentration was 507 mg L^{-1} and the average volumetric sulfate reduction rate was 278 mg L^{-1} d^{-1}. Over 99% precipitation efficiency was achieved for Al, Ni, Co, and Cu using biogenic sulfide and NaOH, accounting for 96% of the metal value contained in the LIB waste leachate. The purity indices of the precipitates were highest for Co, being above 0.7 for the precipitate at pH 10. However, the process was not selective for individual metals due to simultaneous precipitation and the complexity of the metal content of the LIB waste. Overall, the process facilitated the production of high value mixed metal precipitates, which could be purified further or used as feedstock for other processes, such as the production of steel.

Keywords: biogenic hydrogen sulfide; biological sulfate reduction; bioreactor; lithium ion battery; metal precipitation

1. Introduction

Globally, there has been an exponential growth in lithium ion battery (LIB) consumption, with production expected to increase 520% from 2016 to 2020 [1]. LIBs have become an ideal energy storage component for portable devices and electric vehicles (EVs) due to their high energy density and lightweight nature and are expected to dominate the battery market for the next 20 years [2].

Crude recycling and disposal practices of electronic waste (e-waste; such as LIBs) often result in the production of toxic substances (e.g., dioxins) and the leaching of toxic heavy metals into the environment [3–5]. Currently, there are only a few commercial operations capable of recovering metals from LIB waste, largely located in Asia and Europe [6]. In 2012 and 2013, only 2% of LIBs were collected for recycling in Australia, with the remainder still largely disposed of to landfill [2]. Considering the abundance of valuable metals LIBs contain (Table 1) [7], as well as the potentially damaging impact of LIB waste if disposed to the environment, recovering metals from LIB waste is both environmentally and economically attractive.

Table 1. Metals recoverable from LIB waste, along with the percentage composition, commodity prices and total value of metals contained in LIBs (Table modified from [7]). Commodity prices correct as at 13 August 2019 and were sourced from Metalary.

Metal	Metal Content in LIB Waste (%)	Commodity Price ($US/ton)	Metal Value Contained in a ton of LIBs ($US)	Fraction of the Metal Value Contained in a ton of LIBs (%)
Cobalt	20.4	33,000	6732	84.9
Lithium *	2.67	16,500	441	3.3
Nickel	5.42	13,546	734	5.0
Manganese *	1.22	2060	25	0.2
Copper	11.7	5941	695	5.5
Aluminium	6.72	1797	121	1.1
	Total		8748	100

* No daily metal prices available, so the historical commodity price for 2018 was used.

To recover metals from e-waste such as LIBs, the techniques of pyrometallurgy and hydrometallurgy are traditionally employed [8]. Typically, pyrometallurgy is attractive for large-scale operation as LIBs can be processed with other forms of e-waste [9]. The process generally aims to predominantly recover nickel (Ni) and copper (Cu) at high temperatures, which make these processes economically feasible [9]. Therefore, traditional metal recovery processes may not recover all metals associated with complex waste products, such as waste LIB. For example, high temperature treatment does not allow for the recovery of other metals (such as lithium (Li), iron (Fe), aluminium (Al), and manganese (Mn) and the processing can be energy intensive [9].

In comparison, hydrometallurgical processing allows the recovery of most of the metals within LIBs to be extracted, separated and recovered [10]. Leaching of metals from LIB waste have been widely investigated using various lixiviants to promote metal solubilisation [7,11,12]. It has been demonstrated that up to 99% solubilisation of cobalt (Co) and Li can be achieved with LIB wastes using strong inorganic acids such as hydrochloric, sulfuric and nitric acids [9,13,14]. Often in these studies, other recoveries for base metals, Al and Fe are also reported, but the recovery is dependent on the leach conditions implemented for the spent LIB [9]. Similarly, literature demonstrates that between 96% and 100% of Co and Li can be recovered in leach experiments using common organic acids such as citric, succinic and oxalic acids [15–17].

Regardless of the metal solubilisation method employed, the recovery of metals from the complex metal-containing leachate solutions can be challenging. Solutions often contain various metals of complex chemistries and co-digested compounds associated with binders and other materials. Various methods to recover metals from LIB waste have also been investigated including precipitation [18], solvent extraction, [19,20], membrane separation [21] and electrodeposition [22–24]. Using these methods, it has previously been shown that the separation of metal combinations such as Ni and Co and Cu, and Co and Mn are notoriously challenging due their similar chemical and physical properties [18,21].

When combined, these metal extraction and recovery processes are associated with the consumption of large amounts of reagents or high energy inputs. Accordingly, there has been an increasing interest in developing more environmentally benign processes for metal recovery [25–27].

Recently, the recovery of metals from various metal containing waste streams using biogenic sulfide produced by sulfate reducing bacteria (SRB) has been explored as an alternative to the conventional metal precipitation processes [28–31]. In biogenic sulfide generation, the SRB use sulfate as a terminal electron acceptor to oxidise organic compounds or hydrogen to form hydrogen sulfide (Equation (1)) [29]. The hydrogen sulfide gas that is produced is then used to precipitate metals as low solubility metal sulfides (Equation (2)) [29].

$$2CH_2O + SO_4^{2-} \rightarrow H_2S + 2HCO_3^- \quad (1)$$

$$H_2S + M^{2+} \rightarrow MS(s) + 2H^+ \quad (2)$$

The organic substrate (electron donor) is represented by CH_2O. In both Equations (1) and (2), the soluble metal cation is represented by M^{2+}.

Biogenic sulfide precipitation of metals has been demonstrated at scale, with various sulfate- and metal-rich source waters from contaminated and environmental sources, including acid mine drainage, spent refinery waste waters, and final slag leachates [32]. Using sulfide to precipitate metals from low concentration, highly complex, metal containing solutions allows more selective precipitation of target metals as compared to hydroxide precipitation [31], and hence is more beneficial for complex metal containing solutions such as those generated by the leaching of waste LIBs and other e-wastes.

To the best of our knowledge, biogenic sulfide precipitation of metals from LIB waste leach liquors has not yet been investigated. Therefore, this study explored the feasibility of using biogenic sulfide precipitation to recover metals from leach solutions generated from LIB waste. Further, it was anticipated that the use of biogenic sulfide precipitation may provide an alternative pathway for recovering metals from complex metal containing leach liquors generated from other forms of e-waste, such as printed circuit boards and fluorescent lights. As resource recovery is becoming increasingly important for alleviating the environmental impact of e-wastes, the development of alternative resource recovery processes that consume less materials and energy is crucial to assist the transition towards a circular economy for these products.

2. Materials and Methods

2.1. LIB Waste Processing and Composition

Waste LIBs from laptops were collected from a local e-waste processing facility (Total Green Recycling Ltd. Co., Perth, WA, Australia) and were manually dismantled into the plastic housings and battery cells as previously described [7]. Briefly, the battery cells were further processed by course shredding (Shredder Type 600, Kovia Engineering Works, Coimbatore, India) and milling (Essa LM5 mill, FLSmidth, Copenhagen, Denmark). Oversized metal casings were then removed by screening at 16 mm, 10 mm and 5 mm and material <5 mm was re-milled. The particle size fraction of <500 µm was used in the study. The composition of the battery waste (Table 1) was previously determined by X-ray diffraction (XRD) and electron scanning microscopy at CSIRO Mineral Resources Analytical Services Laboratory (Perth, WA, Australia).

2.2. Leaching of LIBs

Processed LIB powder (pulp density 10% *w*/*v*) was leached at 25 °C using 2 N HCl, with shaking at 200 rpm for 24 h. At the completion of leaching, the metal-rich leach solution was recovered by vacuum filtration (0.22 µm) and used for subsequent metal precipitation experiments. The pH and oxidation-reduction potentials (ORP) were recorded at the start and completion of the leaching using a Smart-CHEM meter (Ag/AgCl reference electrode; calibrated with 4.01 and 7.01 standard buffers TPS, Brendale, QLD, Australia). At the completion of leaching, samples were obtained for soluble metals analysis (Al, Ni, Co, Li, Fe, Mg, Mn, Cd, Zn, Cu) by inductively coupled plasma optical emission spectrometry (ICP-OES), undertaken at CSIRO Mineral Resources Analytical Services Laboratory.

2.3. Sulfate Reducing Bioreactor for the Generation of Biogenic Hydrogen Sulfide

2.3.1. Preparation of SRB Inoculum

The sulfate reducing fluidised bed reactor (FBR) was inoculated with a mix of anaerobic SRB cultures previously enriched from various environmental and industrial samples and sourced from the CSIRO Biotechnology Culture Collection. The FBR inoculum was initially enriched with Postgate medium (DSMZ M63, g L^{-1}; K_2HPO_4, 0.5; NH_4Cl, 1.0; Na_2SO_4, 1.0; $MgSO_4{\cdot}7H_2O$, 2.0; $FeSO_4{\cdot}7H_2O$, 0.5; $CaCl_2{\cdot}2H_2O$, 0.1; sodium thioglycolate, 0.1; ascorbic acid; 0.1; yeast extract, 1.0; sodium-DL-lactate,

2.0) to provide a sulfate to lactate mass ratio (sulfate:lactate) of 1:2 [29,33]. Prior to inoculation, the SRBs were cultured on a modified, minimal Postgate medium (g L^{-1}; K_2HPO_4, 0.056; NH_4Cl, 0.111; Na_2SO_4, 1.5; $ZnCl_2$, 0.2; $MgSO4{\cdot}7H_2O$, 1.13; $FeSO_4{\cdot}7H_2O$, 0.28; sodium thioglycolate, 0.011; ascorbic acid; 0.011; sodium-DL-lactate, 0.35; pH was adjusted to 7 if required using 1 M NaOH or 1 M H_2SO_4) so that the sulfate:lactate ratio was 1:0.35 [34].

2.3.2. Bioreactor Operation

The FBR (height 36 cm, internal diameter 5 cm, total volume 0.78 L) and associated sparging reactor (SR) (height 32 cm, internal diameter 5 cm, total volume 0.46 L) had a total liquid volume of 1.24 L (Figure 1). Granular activated carbon (GAC; 0.5–1 mm; 50% *v*/*v*) was added to the FBR as the biomass carrier to facilitate biofilm formation, and the reactor was fluidised between 5% *v*/*v* and 10% *v*/*v* [30,35]. Fluidisation was maintained by recirculation of the bioreactor medium at flow rates determined by the fluidisation rate. Glass beads were placed at the bottom of the reactor to prevent any backflow of the carrier material into the recirculation line.

The FBR was maintained at 35 °C by circulating heated water through tubing wrapped around the reactor, which was also well insulated to minimise heat loss. The FBR was initially operated in batch mode for 15 days to facilitate biofilm formation at the GAC surface. The FBR was then continuously fed with the modified, minimal Postgate medium, at a hydraulic retention time (HRT) between 2.09 days and 2.16 days. The HRT was calculated using the active fluidised bed volume (1.24 L). The pH was monitored continuously by an in-line pH probe (Ionode IJ44A, Tennyson, QLD, Australia; Ag/AgCl reference electrode). The pH of the influent medium was not corrected prior to addition to the reactor and had a starting pH of 4.3. The reactor pH was naturally maintained at approximately 7 because of biogenic alkalinity generation [36,37], but on some occasions when process perturbations were encountered, the pH was manually adjusted to neutral by adding 1 M H_2SO_4 or 1 M NaOH. Microbial activity was measured as dissolved sulfide generation using the colorimetric method described by Cord-Ruwisch [38].

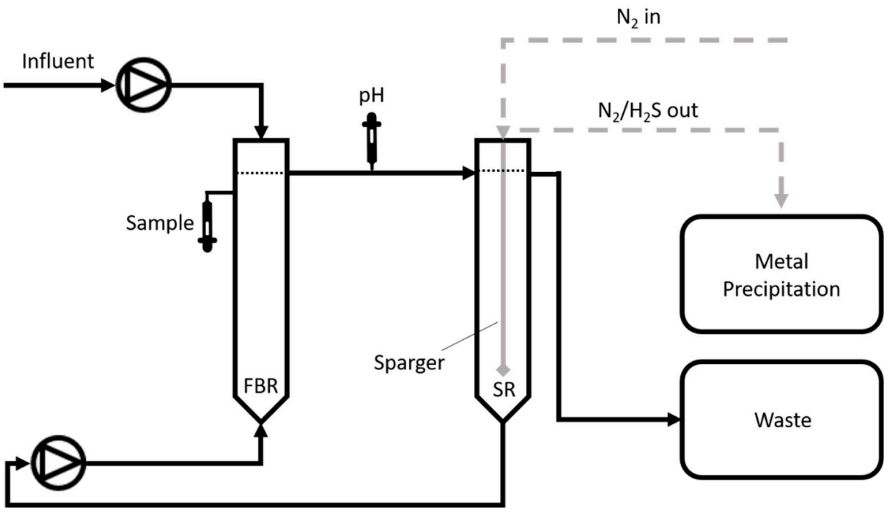

Figure 1. Schematic representation of the fluidised bed reactor (FBR) and sparging reactor (SR) for hydrogen sulfide production and stripping and precipitation of metals from LIB waste leachate. The solution level for each reactor is indicated by the dotted line.

2.4. DNA Extraction and Analysis

Microbial community composition of the FBR was characterised at various times of operation. DNA was extracted from both suspended and attached biomass. Suspended biomass from the bioreactor liquor was collected in a known liquid volume and concentrated prior to DNA extraction. The biomass carrier samples (5 mL) were taken from the fluidised bed. The wet weight of the collected GAC sample was recorded (Table 2), and the samples were sonicated in the bioreactor liquor for three

consecutive 30 s intervals (Ultrasonic bath XUBA3, Grant Instruments, Shepreth, Cambridgeshire, UK) to dislodge the attached biomass from the GAC.

Table 2. Summary of FBR samples analysed for microbial composition in this study.

Sample ID (Day of Operation)	Sample Source	DNA Concentration (ng μL^{-1})	Dissolved Sulfide Concentration in Reactor at the Time of Sampling (mg L^{-1})
A (105)	GAC	2.16	n.d.
B (106)	Concentrated suspension	5.58	n.d.
C (126)	GAC	4.50	762
D (126)	Concentrated suspension	6.92	762
E (146)	GAC	7.68	590
F (147)	Concentrated suspension	6.54	590

n.d. = below the detectable limit.

Cells from both suspended and attached biomass were concentrated to 250 µL by centrifuging at 10,000× *g* for 8 min (Centrifuge 5424R, Eppendorf, Macquarie Park, NSW, Australia). DNA was extracted using the DNeasy Powersoil Kit (Qiagen, Chadstone, VIC, Australia) as per the manufacturer's instructions. The protocol was amended to incubate the membrane filter in elution buffer for an extended period of 10 min before centrifugation. The DNA concentrations were analysed using a Qubit 3.0 Fluorometer (Invitrogen, Thermo Fisher Scientific, Scorseby, VIC, Australia).

DNA samples were mixed in 4:1 ratio with DNA Stable (Sigma-Aldrich, Castle Hill, NSW, Australia) and sent to Molecular Research Laboratory (MR DNA, Shallowater, TX, USA) for sequence analysis using Illumina sequencing. Briefly, DNA was amplified using the HotStarTaq Plus Master Mix Kit (Qiagen) with universal 16S rRNA gene primers, illCUs515F (5'GTGYCAGCMGCCGCGGTAA'3) and new806RB (5'GGACTACNVGGGTWTCTAAT'3). The conditions for amplification were as follows: initial denaturation at 94 °C for 3 min, followed by 30–35 cycles of denaturation at 94 °C for 30 s, primer annealing at 53 °C for 40 s and elongation at 72 °C for 1 min, after which a final elongation step at 72 °C for 5 min was performed. Following amplification, the PCR products were examined on a 2% agarose gel. Samples were purified using calibrated Ampure XP beads. Purified PCR products were used to prepare an Illumina DNA library. Sequencing was performed on a MiSeq following the manufacturer's guidelines. Sequence data was processed using MR DNA's analysis pipeline, and percentage abundance of dominant community members was calculated for both bacterial and archaeal genera in the suspended and attached biomass communities.

2.5. Biogenic Sulfide Precipitation of Metals

The metal-rich leachate (100 mL) was added to a 250 mL precipitation flask and magnetically stirred for the duration of the experiment. During the initial 24 h (Period I), the pH was uncontrolled. Thereafter, the pH of the leach solution was sequentially increased by computer-feedback dosing of 1 M NaOH to two different set-points, namely pH 5 (Period II) and pH 10 (Period III). Feedback control was via a customised LabVIEW program and a controllable peristatic pump (77120-52, Cole Parmer Instrument Company, Vernon Hills, IL, USA).

During the experiment, the SR unit was continuously sparged with an analytical grade N_2 gas at a flow rate of 0.1 L min^{-1}. The recovered H_2S gas was continuously added to the leachate for the duration of the experiment to precipitate metals at each pH set point (Periods I–III). Samples were routinely taken to measure the dissolved sulfide in the FBR [38] and the soluble metal concentrations (ICP-OES) in the precipitation flask. Samples for soluble metal analysis were prepared by membrane filtration (0.22 µm; Merck Millipore, Bayswater, VIC, Australia) before fixing with 7 M HNO_3. During the sparging process, the FBR was maintained in batch mode, and the pH was adjusted to pH 7 using 1 M H_2SO_4, as required.

2.6. Biogenic Sulfide Precipitation Efficiency

The precipitation efficiencies for each metal were calculated using Equation (3), where $[m]_{soluble}$ is the soluble metal concentration [29]:

$$\text{Metal precipitation efficiency (\%)} = ([m]_{soluble} \text{ (before } H_2S \text{ addition)} - [m]_{soluble} \text{ (after } H_2S \text{ addition)}) \times 100/[m]_{soluble} \text{ (before } H_2S \text{ addition)} \quad (3)$$

The purity of metal precipitates obtainable, for each metal, were calculated as purity indices using Equation (4), where m_i is the mass of an individual metal precipitated between pH points, and m_{total} is the mass of all metals precipitated between the same pH points [29]. The mass of metals was calculated based on metal concentrations in solution:

$$\text{Precipitate purity indices} = m/m_{total} \quad (4)$$

3. Results and Discussion

3.1. Bioreactor Performance and Troubleshooting

The FBR performance over a period of approximately 200 days is shown in Figure 2.

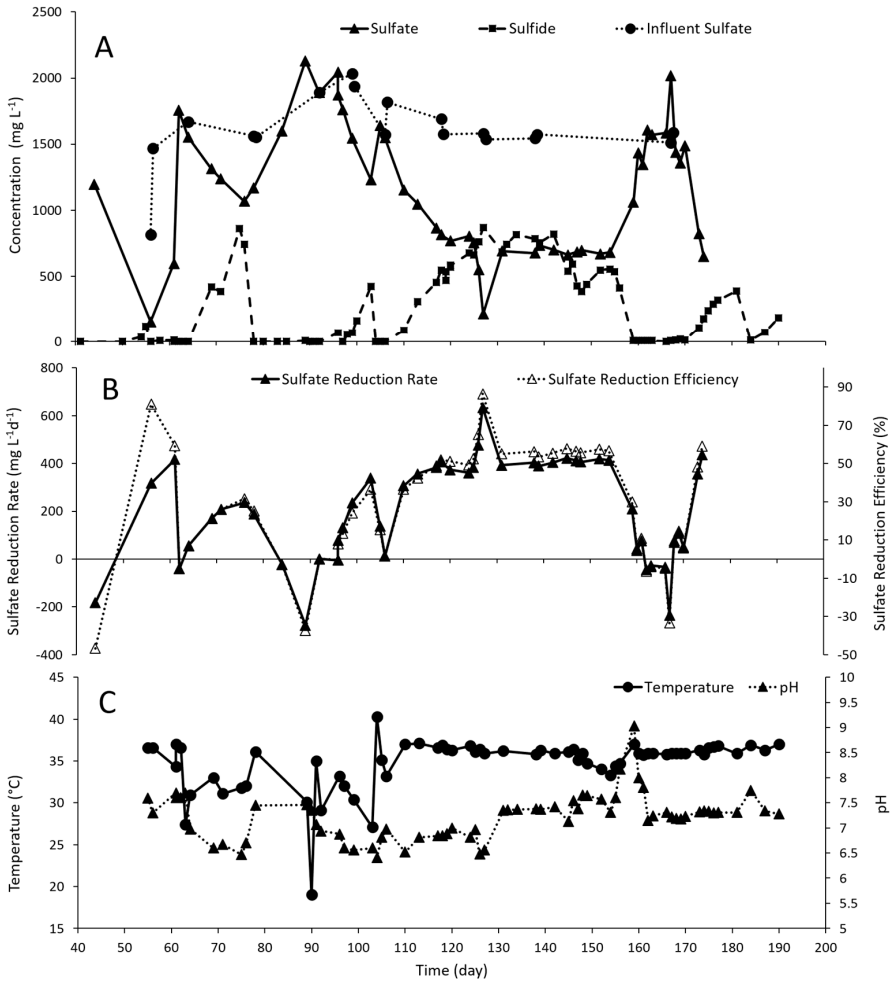

Figure 2. Summary of the sulfidogenic bioreactor performance over the course of the experiment: (**A**) influent sulfate concentration and both sulfide and sulfate concentrations within the bioreactor; (**B**) the rate and efficiency of sulfate reduction within the bioreactor; and (**C**) the temperature and pH of the bioreactor.

In general, the performance varied as reflected by the fluctuations in both the measured dissolved sulfide concentrations and pH. Sulfate reduction rates at times were measured as negative values. This is likely due to the carryover of substrates from inoculum, concentration of sulfate due to evaporation during sparging events and other bioreactor events and/or an artefact of operation of the bioreactor whilst in batch mode.

3.1.1. Dissolved Sulfide, pH and Temperature as Indicators of Microbial Activity

The FBR produced high dissolved sulfide concentrations after approximately two months of operation, reaching a level of up to 860 mg L^{-1} at day 72 (Figure 2A). During periods of sulfide production (dissolved sulfide concentrations >100 mg L^{-1}), the average dissolved sulfide concentration was 507 mg L^{-1}, which is within the typical range reported for sulfidogenic FBRs [30,37,39]. Although this level of dissolved sulfide is close to those reported as inhibitory to SRB (*ca.* 550 mg L^{-1}) [40], it has also been shown that SRB can oxidise substrates at high dissolved sulfide concentrations (up to 1000 mg L^{-1}), albeit at a lower rate [41]. Therefore, the dissolved sulfide concentration achieved by the FBR was considered satisfactory for this work.

During periods of sulfide production, the bioreactor pH and temperature were relatively stable (Figure 2C). However, when the process was not actively producing sulfide (days 90 and 160), notable fluctuations in temperature or pH were recorded, which resulted in delayed recovery of the bioreactor. To expedite the recovery of the bioreactor, the bioreactor was re-inoculated with an active SRB culture on three occasions (on days 61, 92 and 163). Following re-inoculation, the reactor recovered to dissolved sulfide concentration >100 mg L^{-1} within 8–10 days.

3.1.2. Installation of a Separate Sparging Reactor Facilitated Biogenic H_2S Production in the FBR

Prior to installing the sparging reactor (SR; Figure 2: day 104), the sparging device was housed directly within the FBR bed. However, sparging the FBR directly with N_2 gas to strip H_2S resulted in a process failure of the FBR as dissolved sulfide concentration sharply declined (Figure 2: days 61 and 76). The vigorous nature of sparging within the reactor bed may have detached SRB from the carrier material and consequently, the SRB may have been washed out of the reactor system, while bacteria with greater adherence to the carrier material remained [41,42]. The loss of SRB from the bioreactor system would account for the lengthy bioreactor recovery times following sparging events. As the aim of the study was to maximise sulfide generation and not to evaluate the suitability of other biomass carrier materials, the biomass carrier used in this study was not changed to promote stronger attachment of cells. Activate carbon has been reported to be an efficient biomass carrier for FBR [43,44].

To remove H_2S from the reactor without displacing SRB from the biocarrier material, a separate SR was installed in-line with the FBR on day 104 (Figure 1). After installing the SR, two sparging events were carried out (Figure 2: days 155 and 181). Following the sparging on day 155, the bioreactor failed to recover for over 10 days. However, this was due to simultaneous interruption to influent flow, and hence, the likely starvation of the microbial community [34]. The bioreactor performance rapidly increased with no intervention following the sparging event on day 181. This indicated that the use of a separate SR allowed the recovery of H_2S without impacting the activity of the microbial community in the FBR.

3.1.3. Ratio of Sulfate to Lactate was Important for Optimising Sulfide Generation

For the first 56 days of bioreactor operation, the sulfate:lactate mass ratio of the growth medium was 1:2 to enrich and promote biomass growth. However, during this period of operation, only low dissolved sulfide concentrations were recorded, which suggested that growth conditions were not optimal for biogenic sulfide production. The initially low sulfate to lactate ratio may have led to sulfate limitation, allowing acetogens and methanogens to outcompete SRB for substrates [35]. Low sulfate to organic carbon ratio can also result in the accumulation of propionate and acetate in the effluent, which may inhibit sulfidogenisis [34,45,46].

At 56 days, the growth medium was modified to have a sulfate: lactate mass ratio of 1:0.35. Higher sulfate concentrations when compared to lactate have been shown to promote the growth of SRB such as *Desulfovibrio* and *Desulfomicrobium* and is closer to the stoichiometric molar ratio of 3:2 (i.e., mass ratio of 1:0.63) for the complete sulfidogenic oxidation of lactate to bicarbonate (Equation (5)) [29,34]:

$$2CH_3CHOHCOOH + 3SO_4^{2-} \rightarrow 3H_2S + 6HCO_3^- \quad (5)$$

Within 24 h of changing to the modified, minimal Postgate medium, a detectable dissolved sulfide concentration was recorded, and the concentration continued to increase until day 76 when N_2 sparging disrupted the microbial activity (Figure 2: days 61–76). The installation of the SR (day 104), in combination with the use of a minimal, modified Postgate medium allowed the reactor to stabilise over time, and the reactor to recover activity more quickly in times of perturbation.

3.1.4. Sulfate Reduction Rate and Efficiency

During periods of sulfide production (dissolved sulfide concentrations >100 mg L^{-1}), the volumetric sulfate reduction rate varied between 170 and 633 mg L^{-1} d^{-1}, with an average of 378 mg L^{-1} d^{-1} (Figure 2B) and the sulfate reduction efficiency varied between 21% and 86% with an average of 50% (Figure 2B). Although with lower sulfate reduction rates, the sulfate reduction efficiencies were similar to those reported for other FBRs [30,35,37,39,47]. This is likely due to the longer HRT used in this study (2 days), when compared to these other studies. However, Kaksonen et al. [41] indicated that the relationship between sulfate reduction rate and HRT was not linear. Instead, the sulfate reduction rate likely depends on several variables, including sulfate concentration, organic substrate concentration, dissolved sulfide concentration, biomass microbial community, pH and temperature [41]. An increased sulfate reduction rate in the sulfidogenic bioreactor indicated an increased rate of sulfide production. As the bioprecipitation of metals from solution depends on available H_2S, a greater sulfate reduction rate may increase the capacity of sulfidogenic bioreactors for metal recovery.

3.2. Microbial Community Structure

The performance of the FBR was dependent on the microorganisms present, their ability to form consortia on the carrier material and their regeneration capacity [48]. A better understanding of the microbial community present in sulfidogenic bioreactors may provide insight into the reproducibility of this process and the potential to tailor bioreactor conditions for increased performance. In this study, samples for DNA sequencing were taken from both biomass that was suspended in the reactor volume and that attached to the carrier material. The samples were taken 20 days apart during variable bioreactor performance (Table 2). Samples A and B were taken during a period of bioreactor recovery where the dissolved sulfide concentration was undetectable, and the sulfate reduction efficiency was only 1.6%. Samples C and D were taken during an uninterrupted period of sulfide production, when the dissolved sulfide concentration was 762 mg L^{-1} and, the sulfate reduction efficiency was 65%. Finally, samples E and F were taken within 24 h of an interruption to influent flow, when the dissolved sulfide concentration was 590 mg L^{-1} and, the sulfate reduction efficiency was 55%.

The relative abundance data for bacteria and archaea from the suspended biomass samples (Table 2: samples B, D and F) showed minor changes in community composition as bioreactor performance varied. A biofilm consortium can provide a greater resistance to environmental changes compared to a suspended culture [48]. Also, microbes in suspension can easily be washed out from the reactor system [49].

DNA sequencing and relative abundance calculations showed that a diverse, changing and complex bacterial community was present within the FBR (Figure 3; Table 3). Nonetheless, the FBR microbial community, previously enriched from environmental sources and industrial samples, contained common SRB from the genera *Desulfovibrio*, *Desulfomicrobium* and *Desulfococcus*. The most dominant genus present in the bioreactor was *Desulfovibrio* (ranging from 15% to 22%), followed by

Desulfomicrobium (ranging from 8% to 27%), whilst *Desulfococcus* was a minor representative of the SRB community (ranging from 4% to 15%), depending on the sample and time taken from the reactor (Figure 3). These genera have been previously shown to dominate sulfidogenic bioreactors [35,48]. In general, SRB made up between 31% and 58% of the FBR bacterial community, depending on the sampling time (Figure 4).

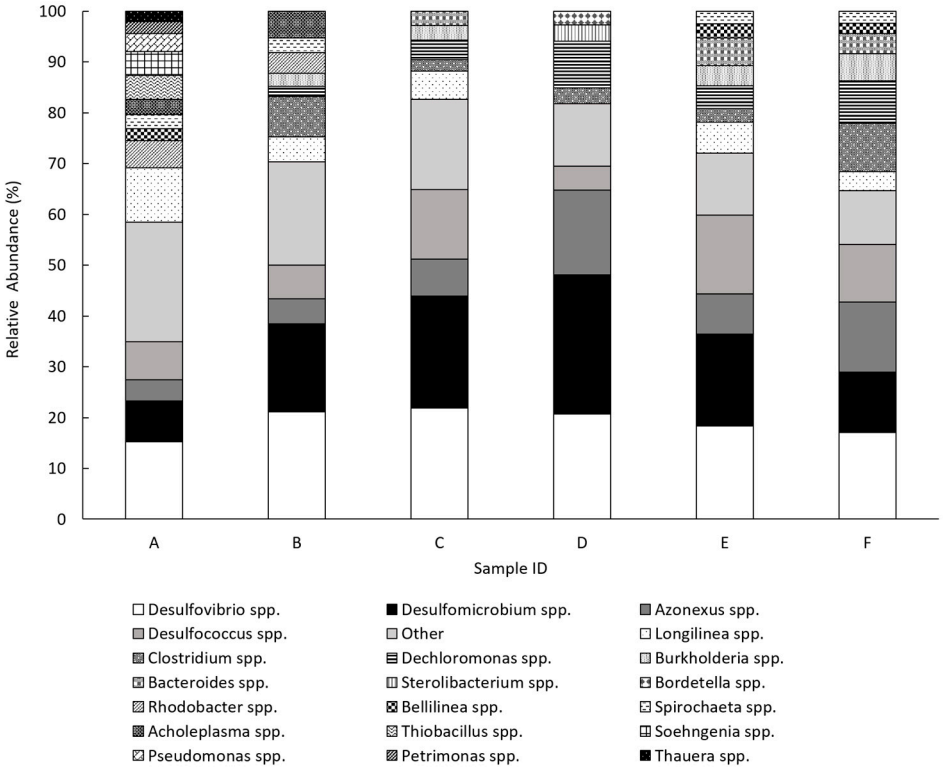

Figure 3. Relative abundance of bacterial genera in the FBR microbial community. Bacterial genera with a relative abundance of <2% are grouped as Other. For detailed description of samples A–F see Table 2.

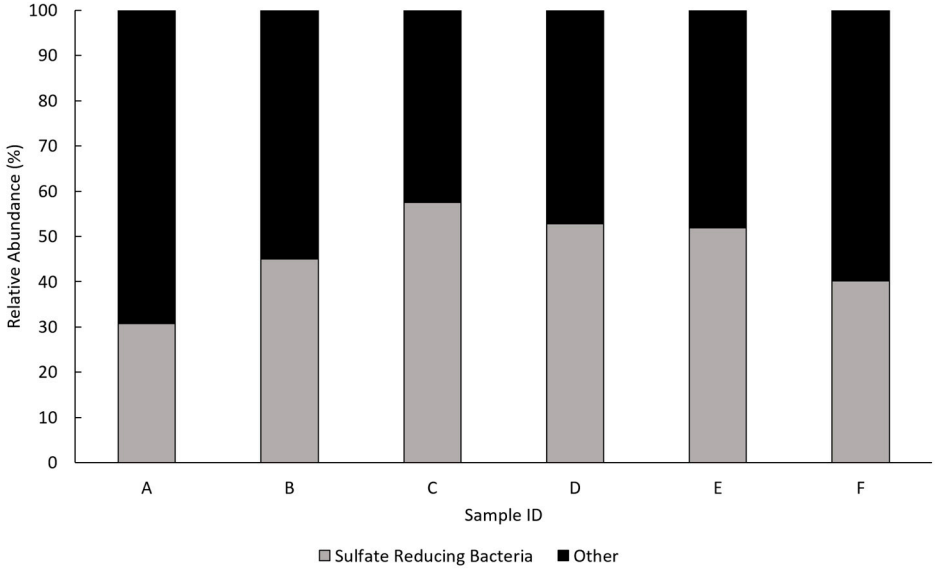

Figure 4. Relative abundance of all sulfate reducing bacteria compared to all bacteria in the microbial community of the sulfidogenic bioreactor. For detailed description of samples A–F see Table 2.

Table 3. Summary of the key bacterial and archaeal genera detected in DNA samples taken from the FBR. All genera listed were present in at least two of the analysed samples and with a relative abundance >2%.

Genus	Sample Detection	Description	References
		Bacteria	
Dechloromonas	B, C, D, E, F	Anaerobic, Gram-negative bacteria capable of complete acetate oxidation by dissimilatory (per)chlorate reduction to chloride.	[50,51]
Clostridium	B, C, D, E, F	A diverse genus of anaerobic, spore forming, Gram-positive bacteria found in soils, animals and humans (both pathogenically and commensally).	[52]
Longilinea	A, B, C, E, F	Anaerobic Gram-negative bacteria which utilise proteins and some sugars for growth. Growth is enhanced in co-culture with hydrogen scavenging methanogens.	[53,54]
Bellilinea	A, E, F	Anaerobic Gram-negative bacteria which utilise carbohydrates for growth. Growth is enhanced in co-culture with hydrogen scavenging methanogens.	[54]
Desulfovibrio	All	Anaerobic Gram-negative SRB. They incompletely oxidise organic substrates to acetate.	[55–57]
Desulfomicrobium	All	Anaerobic Gram-negative SRB. They incompletely oxidise organic substrates to acetate.	[58,59]
Azonexus	All	Facultative aerobic Gram-negative bacteria. Capable of nitrogen fixation.	[60,61]
Desulfococcus	All	Strictly anaerobic Gram-negative SRB. They completely oxidise organic substrates.	[62–64]
Rhodobacter	A, B	Gram-negative bacteria with a range of metabolic capabilities. Main species of this genus are photosynthetic purple bacteria.	[65,66]
Spirochaeta	A, B, E, F	Anaerobic, saccharolytic and helical shaped bacteria.	[67,68]
Acholeplasma	A, B	Wall-less bacteria with uncertain classifications as either saprotrophic or pathogenic.	[69]
Bacteroides	C, E, F	Anaerobic Gram-negative bacteria largely found in the mammalian gastrointestinal microbiota. They break down complex molecules (such as plant and host-derived glycans) to simpler ones.	[70,71]
Burkholderia	B, C, E, F	Gram-negative bacteria which are aerobic but can often tolerate anaerobic conditions. They include animal, human and plant pathogens, as well as environmentally important species involved in nitrogen fixation, promoting plant growth and killing pest organisms.	[72,73]
		Archaea	
Methanobacterium	All	Methanogenic archaea known to grow on hydrogen and carbon dioxide. They grow without oxygen and are often present in anaerobic bioreactors. They exhibit similar growth kinetics to *Desulfovibrio.*	[74,75]
Methanosarcina	A, C, E	Archaeal genus containing species of acetoclastic methanogens that play a pivitol role in anaerobic consortia.	[76]
Thermogymnomonas	C, E	Aerobic, acidophilic and heterotrophic archaea which lack a cell wall.	[77]

The FBR archaeal community consisted mainly of H_2- and CO_2-utilising methanogens, belonging to the genus *Methanobacterium*. This genus comprised between 88% and 94% of the archaeal community of the attached biomass taken from the FBR carrier samples (Table 2: samples A, C, and E). The carrier samples contained multiple genera of methanogenic archaea (Table 2). A much less diverse archaeal community was observed in the suspended biomass samples (Table 2: samples B, D, and F). The diversity of the archaeal community (in the carrier samples) showed that methanogenic archaea adhered to the carrier material [74]. The presence of methanogenic archaea in the attached biomass consortium indicated that the conditions within the FBR were conducive for the growth of methanogens, which may in turn affect the activity of the SBR for sulfate reduction [53,54]. Microbial community analysis also showed that the FBR contained many non-SRB (Figure 4; Table 3). It is likely that some non-SRB were responsible for degrading complex organic matter produced by the biocarrier consortium, providing additional energy and carbon sources, or nutrients (e.g., nitrogen source) for the SRB [41]. *Azonexus* and *Desulfococcus* were most abundant within 24 h of an interruption to influent flow (Figure 3: sample E at day 146). This suggested that when there is a lack of available substrates for growth nutrients, *Azonexus* and *Desulfococcus* remain attached to the carrier material. In contrast, SRB such as *Desulfovibrio* and *Desulfomicrobium* are more likely to detach and wash out from the bioreactor [48].

Four genera, namely *Clostridium*, *Dechloromonas*, *Burkholderia* and *Bacteroides* were only detected at a relative abundance of <10% when the reactor was producing sulfide (Figure 3). Bacterial genera of low abundance may still play a pivotal role in maintaining a stable consortium and supporting the growth of SRB by contributing to nutrient cycling and removal of secondary substrates and metabolites [50,52] (Table 3). Members of the genus *Longilinea* were least abundant when the bioreactor was experiencing uninterrupted sulfide production and most abundant during bioreactor recovery. The growth of *Longilinea* is often supported by methanogens, which can outcompete SRB under certain conditions [53,54]. The abundance of *Longilinea* may indicate unfavourable bioreactor conditions for SRB and an abundance of methanogens. The number of genera detected at relative abundance of less than 2%, decreased by 5.8% between samples A and C (21 days) and 5.6% between samples C and E (20 days) (Figure 3). This suggested that over time, the diversity of the microbial community decreased.

3.3. Metal Sulfide Precipitation

3.3.1. Sparging by the SR Immediately Removed All H_2S, but the FBR Remained Active

Sulfide speciation in solution is dependent on pH. The dominant sulfide form in acidic solution (pH < 7) is H_2S, whereas the dominant form becomes HS^- in an alkaline solution (pH > 7) [31]. Since the experiment required the removal of H_2S from the bioreactor, it was critical that reactor pH was maintained at pH not exceeding 7. Figure 5A shows that bioreactor pH increased gradually following N_2 sparging, due to H^+ removal from solution as H_2S forms (Equation (6)). During the precipitation experiment, the reactor pH was manually lowered with 1 M H_2SO_4 to increase the dissolved H_2S concentration, facilitating the stripping of H_2S to the gas phase for precipitating metals from the leach solution:

$$H^+ + HS^- \rightarrow H^2S \quad (6)$$

The precipitation experiment ran for 75 h with continuous sparging of the SR. Figure 5A shows that the dissolved sulfide concentration of the bioreactor decreased rapidly to undetectable levels at the start of Period II. At the end of Period I, the leachate was filtered to remove any precipitates. Throughout Period II, the leachate became noticeably turbid and darkened in appearance as metal sulfides continued to precipitate from solution. Although dissolved sulfide concentrations had decreased to undetectable levels, the SRB had remained metabolically active. However, as soon as the SRB produced H_2S, it was stripped from the SR by the N_2 gas sparging. This would account for the undetectable dissolved sulfide concentrations observed for the remainder of the experiment. A dissolved sulfide concentration of 10 mg L^{-1} was recorded shortly after the end of the experiment, further indicating that the SRB was metabolically active (Figure 5A: ~73 h).

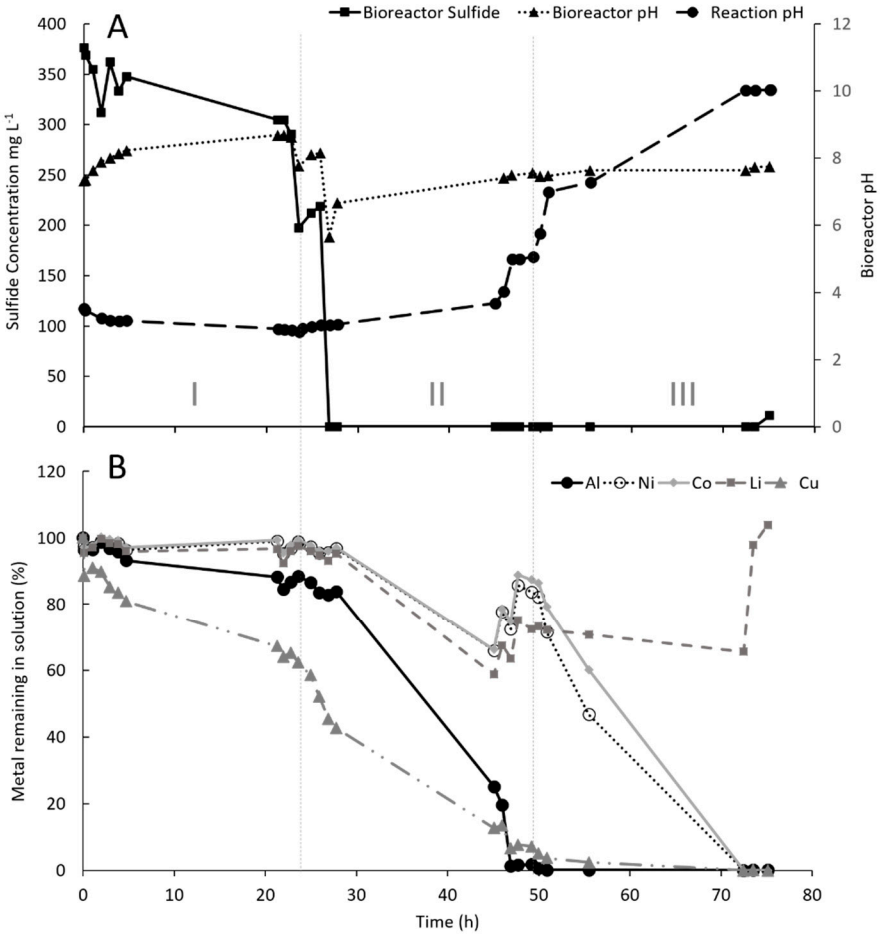

Figure 5. Results of the bio-precipitation experiment: (**A**) Bioreactor dissolved sulfide concentration, bioreactor pH and leach solution pH; and (**B**) Precipitation efficiencies of the most abundant metals in LIB waste. Experimental periods were: uncontrolled pH (Period I), increasing to pH 5 (Period II) and then pH 10 (Period III), as indicated by the vertical dotted lines.

3.3.2. Recovery of Metals was pH Dependent

The H_2S produced in the sulfidogenic bioreactor was used to precipitate and recover metals from the LIB waste leachate. Biogenic sulfide was added to the leachate via gas sparging, as opposed to directly adding the sulfide containing effluent from the bioreactor, as practiced in previous studies [30]. The use of gas transfer was favored in this study as it may enable better pH control for metal recovery than when using bioreactor effluent for precipitation. The leach solution had an initial pH of 3.5, and this continued to spontaneously decrease with the addition of H_2S and without pH control in Period I (Figure 5A), likely due to the formation of copper sulfide (Equation (7)):

$$H_2S + Cu^{2+} \rightarrow CuS(s) + 2H^+ \quad (7)$$

In Period I, 38% Cu and 12% Al were precipitated, while other metals remained largely in solution (Figure 5B). Soon after the addition of H_2S to the leachate, the color of the solution changed from a transparent pink-red to a turbid black-brown, which indicated the formation of metal sulfides. By the end of Period II, Cu and Al had precipitated from solution at efficiencies of 93% and 98%, respectively. Li, Ni and Co appeared to precipitate slightly, but efficiencies were low and variable throughout this period of precipitation (Figure 5B). At the end of Period III, Ni (99.9%), Co (99.9%), Mn (98.9%), Cd (98.6%) and Zn (98.4%) precipitated from solution, which indicated that a complex metal precipitate was formed as the pH was increased to a set point of 10 (Figure 5A,B). Cibati et al. [29] and

Kaksonen et al. [30] also reported low precipitation efficiencies for Ni and Co as sulfides within the pH ranges as recorded in Periods I and II. The low precipitation efficiencies for Ni and Co until Period III showed that increasing the leachate pH to 10 was essential to recover most of these metals. Based on solution analysis alone, it was not possible to determine if the metals had precipitated as metal sulfides or hydroxides at more alkaline pH values.

As shown in Table 4, all metals had precipitated from solution at efficiencies greater than 98% at the end of the experiment (pH 10), except for magnesium (49%) and lithium (0%). Mg does not readily precipitate as a sulfide, and MgS spontaneously decomposes in aqueous systems. The precipitation of Mg observed in this study is likely to be attributed to the precipitation of MgO_2 and $Mg(OH)_2$, which occurs over a range of pH 8 to 14 in aqueous systems as shown by the Mg Pourbaix diagram [78]. The precipitation efficiency of Li reached percentages greater than 30% at times throughout the precipitation experiment. However, by the conclusion of the experiment all the precipitated lithium had returned to solution. This may be explained by the high solubility of lithium sulfide or the reaction of lithium sulfide with HCl, producing H_2S (Equation (8)):

$$Li_2S + 2HCl \rightarrow 2LiCl + H_2S \quad (8)$$

Lithium does not precipitate as a metal sulfide within the pH range used in this study. Therefore, other methods, such as metal carbonate precipitation, are necessary to adequately recover lithium from the leachate solution. For instance, Meshram et al. [79] successfully recovered Li from LIB waste leachate as lithium carbonate (98% purity) upon the addition of sodium carbonate (pH 14). Hence, it is likely that the recovery of Li. This process is beneficial as it results in the production of a lithium-rich solution that can be further processes to recover lithium for secondary use. Recovery of lithium will require an additional carbonation or hydroxide precipitation step after the sulfide precipitation of other metals from solution.

Table 4. Initial concentration of metals in LIB waste leachate and precipitation efficiencies (pH 10).

Metal	Initial Leachate Metals (mg L^{-1})	Precipitation Efficiency (%)
Al	5420	99.9
Ni	4160	99.9
Co	17,400	99.9
Li	2470	0.00
Fe	1140	99.5
Mg	34.6	49.1
Mn	987	98.9
Cd	91.3	98.6
Zn	78.7	98.4
Cu	9600	99.9

3.3.3. Purity Indices of Metal Precipitates

The ability to selectively recover metals with H_2S was assessed by calculating the purity indices for each metal as selected pH values (Figure 6) [29]. The purity index illustrates the relative amount of each individual metal precipitated from solution between pH points. For example, 35% of the total metal precipitated at a pH of 3 was Cu (shown in Figure 6 as a purity index of 0.35 at pH 3). The highest purity index detected was 0.75 for Co between pH 7 and pH 10. The highest purity indices for Cu and Ni were obtained at pH between 5 and 7, namely 0.42 and 0.31, respectively, whereas the highest purity index of 0.29 for Al was recorded at pH between 4 and 5. The results also suggested that the biogenic

sulfide precipitation of metals from LIB waste leachate was not truly selective, as multiple metals were precipitated from solution at all pH values tested (Figure 6). Nonetheless, relatively high purity indices for Co (0.75 at pH 7–10) and Cu (0.42 at pH 5–7) were calculated. This is significant because Co and Cu make up 90.4% of the metal value contained in LIBs (Table 1). The similar precipitation properties of Ni and Co make it difficult for high purity Ni to be selectively recovered [29]. The majority of Al precipitated between pH 3 and 5, which was when most metals began to precipitate from solution, making it difficult to selectively recover high purity Al. Al precipitation in the acidic pH range could likely be attributed to the precipitation of hydroxysulfate minerals, as described by Falagan et al. [80]. However, in the alkaline pH range, Al precipitation is more likely to be in the form of $Al(OH_2)$ [78]. Finally, the precipitation of Li proved difficult due to the solubility and reactivity of lithium sulfide in the leachate, as previously discussed (Equation (7)).

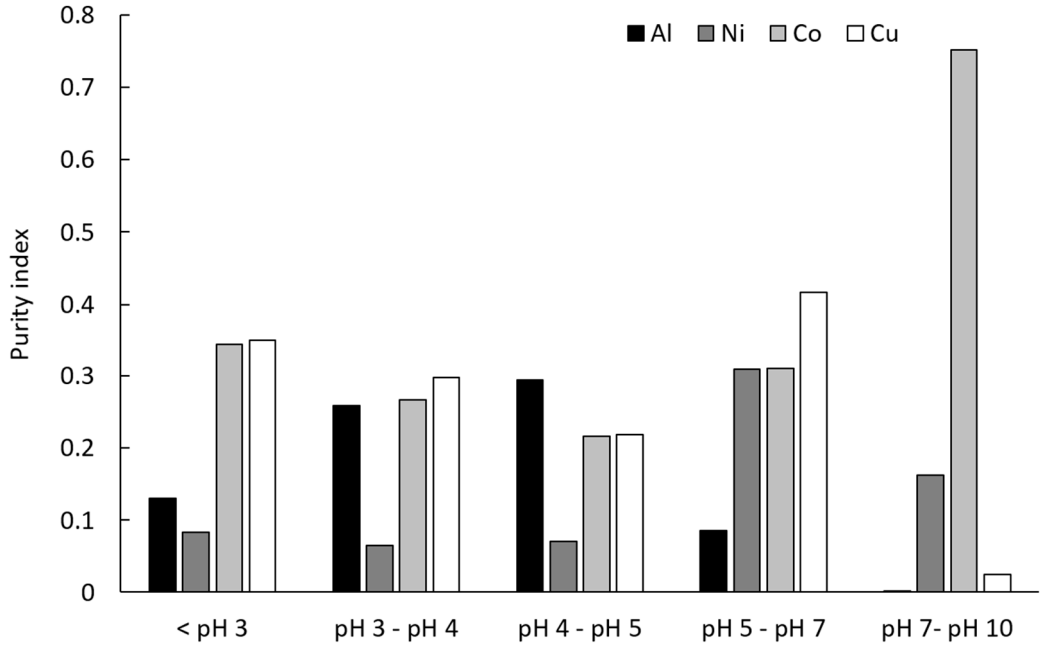

Figure 6. Purity indices for key metals in metal precipitates. Calculated based on the mass of metal precipitated between each pH value shown (Equation (4)).

3.4. Implications of Findings

Some previous studies have investigated the selective precipitation of metals using biogenic sulfide [29]. However, the use of biogenic sulfide for precipitating metals from waste LIB leach liquors has to our knowledge not been previously demonstrated. The precipitation efficiencies of Cu and Zn in this study are in line with those reported previously for sulfidogenic FBR metal recovery processes [30,39]. The present study also showed Al, Co, Ni, and Fe precipitating at efficiencies over 99%, in line with the findings of Sahinkaya et al. [81]. However, it should also be noted that the initial metal concentrations in this study (Table 4) were much higher than the concentrations used in the previously mentioned studies. The purity indices for individual metals reported by Cibati et al. [29], were much higher than those obtained from this study. However, the present study attempted to recover a greater number of metals (10) from a leach solution than Cibati et al. [29] (four metals only) and some other mixed metal precipitation studies [48,82].

The metals obtained from solution in this study were not selectively separated. There is an opportunity to optimise this process to promote selective metal separation, and this can potentially be achieved by refining the pH set points, reagent concentrations, scale and time course of the experiment. Nonetheless, it is anticipated that the separation of metals such as Co, Cu, Mn and Ni will remain a challenge due to their similar chemical and physical properties [29]. The present

study demonstrated that high purity metal sulfide mixtures could be generated, and these can potentially be further refined into high value alloys. Since Al, Ni, Co and Cu represent over 96% of the metal value contained in LIB waste, it was concluded that most of the metal value of LIB waste can be successfully recovered with biogenic sulfide precipitation as demonstrated in this study. However, further techno-economic assessment is required to quantify costs associated with processing, and identify potential end uses for the mixed metal sulfide products generated.

4. Conclusions

Biogenic hydrogen sulfide produced in the FBR and an incremental pH increase to 10 with NaOH, precipitated Al, Ni, Co, and Cu at recovery efficiencies greater than 98%, resulting in high (96%) recovery of the metal value from LIB waste. The purity indices were highest for Co and Cu, achieving 0.75 at pH 10 and, 0.42 at pH 7, respectively. The mixed metal sulfides produced by non-selective biogenic sulfide precipitation could be further refined for the manufacture of high value metal products, but further process optimisation for improving metal recovery selectivity and purity of the mixed metal sulfides is required. The economic feasibility of this process for the recovery of mixed metals from waste streams also needs to be further investigated. Additional work to analyse metal precipitates generated would provide further insight to the mechanism of metal precipitation using biogenic sulfide precipitation as the recovery method.

Author Contributions: Conceptualization, N.J.B., A.H.K., and K.Y.C.; methodology, G.C., J.V.Y. and N.J.B.; formal analysis, G.C. and N.J.B.; investigation, G.C. and N.J.B.; data curation, G.C.; writing—original draft preparation, G.C. and N.J.B.; writing—review and editing, G.C., N.J.B., A.H.K., K.Y.C., J.V.Y. and B.C.; visualization, G.C.; supervision, N.J.B., A.H.K., and K.Y.C.; project administration, N.J.B; funding acquisition, N.J.B., A.H.K., and K.Y.C.

Funding: This research received no external funding.

Acknowledgments: The authors acknowledge the CSIRO Research Office, CSIRO Land and Water, Murdoch University Postgraduate Office for providing some funding this work. This project has also been assisted by the New South Wales Government through its Environmental Trust. The authors thank Christina Morris for her assistance with the molecular work and general laboratory guidance, and Himel Nahreen Khaleque and Geoffrey Puzon (CSIRO Land and Water) for reviewing the manuscript prior to submission.

Conflicts of Interest: The authors declare no conflict of interest.

References

1. Desjardins, J. China Leading the Charge for Lithium-Ion Megafactories. Available online: https://www.mining.com/web/china-leading-the-charge-for-lithium-ion-megafactories/ (accessed on 13 August 2019).
2. Randell, P. *Waste Lithium-Ion Battery Projections*; Final Report; Department of the Environment and Energy: Canberra, Australia, 2016.
3. Hong, Y.; Valix, M. Bioleaching of electronic waste using acidophilic sulfur oxidising bacteria. *J. Clean. Prod.* **2014**, *65*, 465–472. [CrossRef]
4. Ibietela, D.; Eucharia Uche, N. Effect of Spent Laptop Battery Waste on Soil Microorganisms. *Int. J. Curr. Microbiol. Appl. Sci.* **2016**, *5*, 867–876. [CrossRef]
5. Yu, Y.; Chen, B.; Huang, K.; Wang, X.; Wang, D. Environmental impact assessment and end-of-life treatment policy analysis for Li-ion batteries and Ni-MH batteries. *Int. J. Environ. Res. Public Health* **2014**, *11*, 3185–3198. [CrossRef] [PubMed]
6. Heelan, J.; Gratz, E.; Zheng, Z.; Wang, Q.; Chen, M.; Apelian, D.; Wang, Y. Current and Prospective Li-Ion Battery Recycling and Recovery Processes. *JOM* **2016**, *68*, 2632–2638. [CrossRef]
7. Boxall, N.J.; Adamek, N.; Cheng, K.; Haque, N.; Bruckard, W.; Kaksonen, A. Multistage leaching of metals from spent lithium ion battery waste using electrochemically generated acidic lixiviant. *Waste Manag.* **2018**, *74*, 435–445. [CrossRef]
8. King, S.; Boxall, N. Lithium battery recycling in Australia: Defining the status and identifying opportunities for the development of a new industry. *J. Clean. Prod.* **2019**, *215*, 1279–1287. [CrossRef]
9. Pagnanelli, F.; Moscardini, E.; Altimari, P.; Abo Atia, T.; Toro, L. Cobalt products from real waste fractions of end of life lithium ion batteries. *Waste Manag.* **2016**, *51*, 214–221. [CrossRef]

10. Sun, L.; Qiu, K. Organic oxalate as leachant and precipitant for the recovery of valuable metals from spent lithium-ion batteries. *Waste Manag.* **2012**, *32*, 1575–1582. [CrossRef]
11. Dolker, T.; Pant, D. Bioremediation of metals from lithium-ion battery (LIB) waste. In *Waste Bioremediation*; Springer: Berlin/Heidelberg, Germany, 2018; pp. 265–278.
12. Lv, W.; Wang, Z.; Cao, H.; Zheng, X.; Jin, W.; Zhang, Y.; Sun, Z. A sustainable process for metal recycling from spent lithium-ion batteries using ammonium chloride. *Waste Manag.* **2018**, *79*, 545–553. [CrossRef]
13. Jha, M.K.; Kumari, A.; Jha, A.K.; Kumar, V.; Hait, J.; Pandey, B.D. Recovery of lithium and cobalt from waste lithium ion batteries of mobile phone. *Waste Manag.* **2013**, *33*, 1890–1897. [CrossRef]
14. Li, J.; Shi, P.; Wang, Z.; Chen, Y.; Chang, C.C. A combined recovery process of metals in spent lithium-ion batteries. *Chemosphere* **2009**, *77*, 1132–1136. [CrossRef] [PubMed]
15. Li, L.; Zhai, L.; Zhang, X.; Lu, J.; Chen, R.; Wu, F.; Amine, K. Recovery of valuable metals from spent lithium-ion batteries by ultrasonic-assisted leaching process. *J. Power Sources* **2014**, *262*, 380–385. [CrossRef]
16. Zeng, X.; Li, J.; Shen, B. Novel approach to recover cobalt and lithium from spent lithium-ion battery using oxalic acid. *J. Hazard. Mater.* **2015**, *295*, 112–118. [CrossRef] [PubMed]
17. Li, L.; Qu, W.; Zhang, X.; Lu, J.; Chen, R.; Wu, F.; Amine, K. Succinic acid-based leaching system: A sustainable process for recovery of valuable metals from spent Li-ion batteries. *J. Power Sources* **2015**, *282*, 544–551. [CrossRef]
18. Lupi, C.; Pasquali, M. Electrolytic nickel recovery from lithium-ion batteries. *Miner. Eng.* **2003**, *16*, 537–542. [CrossRef]
19. Chagnes, A.; Pospiech, B. A brief review on hydrometallurgical technologies for recycling spent lithium-ion batteries. *J. Chem. Technol. Biotechnol.* **2013**, *88*, 1191–1199. [CrossRef]
20. Granata, G.; Moscardini, E.; Pagnanelli, F.; Trabucco, F.; Toro, L. Product recovery from Li-ion battery wastes coming from an industrial pre-treatment plant: Lab scale tests and process simulations. *J. Power Sources* **2012**, *206*, 393–401. [CrossRef]
21. Baba, Y.; Kubota, F.; Goto, M.; Cattrall, R.; Kolev, S.P. Separation of cobalt(II) from manganese(II) using a polymer inclusion membrane with N-[N,N-di(2-ethylhexyl)aminocarbonylmethyl]glycine (D2EHAG) as the extractant/carrier. *J. Chem. Technol. Biotechnol.* **2016**, *91*, 1320–1326. [CrossRef]
22. Garcia, E.M.; Taroc, H.A.; Matencio, T.; Domingues, R.Z.; dos Santos, J.A.F.; de Freitas, M. Electrochemical recycling of cobalt from spent cathodes of lithium-ion batteries: Its application as coating on SOFC interconnects. *J. Appl. Electrochem.* **2011**, *41*, 1373–1379. [CrossRef]
23. Freitas, M.; Celante, V.G.; Pietre, M.K. Electrochemical recovery of cobalt and copper from spent Li-ion batteries as multilayer deposits. *J. Power Sources* **2010**, *195*, 3309–3315. [CrossRef]
24. Freitas, M.; Garcia, E.M. Electrochemical recycling of cobalt from cathodes of spent lithium-ion batteries. *J. Power Sources* **2007**, *171*, 953–959. [CrossRef]
25. Niu, Z.; Zou, Y.; Xin, B.; Chen, S.; Liu, C.; Li, Y. Process controls for improving bioleaching performance of both Li and Co from spent lithium ion batteries at high pulp density and its thermodynamics and kinetics exploration. *Chemosphere* **2014**, *109*, 92–98. [CrossRef]
26. Zeng, G.; Deng, X.; Luo, S.; Luo, X.; Zou, J. A copper-catalyzed bioleaching process for enhancement of cobalt dissolution from spent lithium-ion batteries. *J. Hazard. Mater.* **2012**, *199*, 164–169. [CrossRef]
27. Mishra, D.; Kim, D.J.; Ralph, D.E.; Ahn, J.G.; Rhee, Y.H. Bioleaching of metals from spent lithium ion secondary batteries using *Acidithiobacillus ferrooxidans*. *Waste Manag.* **2008**, *28*, 333–338. [CrossRef]
28. Cao, J.; Zhang, G.; Mao, Z.; Fang, Z.; Yang, C. Precipitation of valuable metals from bioleaching solution by biogenic sulfides. *Miner. Eng.* **2008**, *22*, 289–295. [CrossRef]
29. Cibati, A.; Cheng, K.; Morris, C.; Ginige, M.; Sahinkaya, E.; Pagnanelli, F.; Kaksonen, A. Selective precipitation of metals from synthetic spent refinery catalyst leach liquor with biogenic H_2S produced in a lactate-fed anaerobic baffled reactor. *Hydrometallurgy* **2013**, *139*, 154–161. [CrossRef]
30. Kaksonen, A.H.; Lavonen, L.; Kuusenaho, M.; Kolli, A.; Närhi, H.; Vestola, E.; Puhakka, J.; Tuovinen, O.H. Bioleaching and recovery of metals from final slag waste of the copper smelting industry. *Miner. Eng.* **2011**, *24*, 1113–1121. [CrossRef]
31. Kaksonen, A.H.; Puhakka, J. Sulfate reduction based bioprocesses for the treatment of acid mine drainage and the recovery of metals. *Eng. Life Sci.* **2007**, *7*, 541–564. [CrossRef]

32. Kaksonen, A.H.; Boxall, N.J.; Gumulya, Y.; Khaleque, H.N.; Morris, C.; Bohu, T.; Cheng, K.Y.; Usher, K.; Lakaniemi, A.M. Recent progress in biohydrometallurgy and microbial characterisation. *Hydrometallurgy* **2018**, *180*, 7–25. [CrossRef]
33. Campbell, L.; Postgate, J. Revision of the holotype strain of *Desulfotomaculum ruminis* (Coleman) Campbell and Postgate. *Int. J. Syst. Evol. Microbiol.* **1969**, *19*, 139–140. [CrossRef]
34. Dar, S.; Kleerebezem, R.; Stams, A.; Kuenen, J.; Muyzer, G. Competition and coexistence of sulfate-reducing bacteria, acetogens and methanogens in a lab-scale anaerobic bioreactor as affected by changing substrate to sulfate ratio. *Appl. Microbiol. Biotechnol.* **2008**, *78*, 1045–1055. [CrossRef]
35. Kaksonen, A.H.; Riekkola-Vanhanen, M.; Puhakka, J. Optimization of metal sulphide precipitation in fluidized-bed treatment of acidic wastewater. *Water Res.* **2003**, *37*, 255–266. [CrossRef]
36. McMahon, M. Development of a Sulfate Reducing Packed Bed Bioreactor for Use in a Sustainable Hydrogen Production Process. Master's Thesis, Queen's University, Kingston, ON, Canada, 2007.
37. Ucar, D.; Bekmezci, O.; Kaksonen, A.; Sahinkaya, E. Sequential precipitation of Cu and Fe using a three-stage sulfidogenic fluidized-bed reactor system. *Miner. Eng.* **2011**, *24*, 1100–1105. [CrossRef]
38. Cord-Ruwisch, R. A quick method for the determination of dissolved and precipitated sulfide in cultures of sulfate-reducing bacteria. *J. Microbiol. Meth.* **1985**, *4*, 33–36. [CrossRef]
39. Sahinkaya, E.; Gungor, M. Comparison of sulfidogenic up-flow and down-flow fluidized-bed reactors for the biotreatment of acidic metal-containing wastewater. *Bioresour. Technol.* **2010**, *101*, 9508–9514. [CrossRef]
40. Reis, M.; Almeida, J.; Lemos, P.; Carrondo, M. Effect of hydrogen sulfide on growth of sulfate reducing bacteria. *Biotechnol. Bioeng.* **1992**, *40*, 593–600. [CrossRef]
41. Kaksonen, A.; Franzmann, P.; Puhakka, J. Effects of hydraulic retention time and sulfide toxicity on ethanol and acetate oxidation in sulfate-reducing metal-precipitating fluidized-bed reactor. *Biotechnol. Bioeng.* **2004**, *86*, 332–343. [CrossRef]
42. Harada, H.; Uemura, S.; Momonoi, K. Interaction between sulfate-reducing bacteria and methane-producing bacteria in UASB reactors fed with low strength wastes containing different levels of sulfate. *Water Res.* **1994**, *28*, 355–367. [CrossRef]
43. Özkaya, B.; Kaksonen, A.H.; Sahinkaya, E.; Puhakka, J.A. Fluidized bed reactor biotechnology for multiple environmental engineering solutions. *Water Res.* **2019**, *150*, 452–465. [CrossRef]
44. Van der Meer, T.; Kinnunen, P.H.M.; Kaksonen, A.H.; Puhakka, J.A. Effect of fluidized-bed carrier material on biological ferric sulphate generation. *Miner. Eng.* **2007**, *20*, 782–792. [CrossRef]
45. McCartney, D.; Oleszkiewicz, J. Competition between methanogens and sulfate reducers: Effect of COD:sulfate ratio and acclimation. *Water Environ. Res.* **1993**, *65*, 655–664. [CrossRef]
46. Mendez, R.; ten Brummeler, E.; Hulshoffpol, L. Start up of UASB reactors treating sucrose containing substrates with low COD/sulfate ratio. *Environ. Technol. Lett.* **1989**, *10*, 83–90. [CrossRef]
47. Bertolino, S.; Silva, L.; Aquino, S.; Leão, V. Comparison of UASB and fluidized-bed reactors for sulfate reduction. *Braz. J. Chem. Eng.* **2015**, *32*, 59–71. [CrossRef]
48. Kiran, M.; Pakshirajan, K.; Das, G. An overview of sulfidogenic biological reactors for the simultaneous treatment of sulfate and heavy metal rich wastewater. *Chem. Eng. Sci.* **2017**, *158*, 606–620. [CrossRef]
49. Marin, P.; Alkalay, D.; Guerrero, L.; Chamy, R.; Schiappacasse, M. Design and startup of an anaerobic fluidized bed reactor. *Water Sci. Technol.* **1999**, *40*, 63–70. [CrossRef]
50. Achenbach, L.; Michaelidou, U.; Bruce, R.; Fryman, J.; Coates, J. Dechloromonas agitata gen. nov., sp. nov. and Dechlorosoma suillum gen. nov., sp. nov., two novel environmentally dominant (per) chlorate-reducing bacteria and their phylogenetic position. *Int. J. Syst. Evol. Microbiol.* **2001**, *51*, 527–533. [CrossRef]
51. Wolterink, A.; Kim, S.; Muusse, M.; Kim, I.; Roholl, P.; van Ginkel, C.; Kengen, S. Dechloromonas hortensis sp. nov. and strain ASK-1, two novel (per) chlorate-reducing bacteria, and taxonomic description of strain GR-1. *Int. J. Syst. Evol. Microbiol.* **2005**, *55*, 2063–2068. [CrossRef]
52. Collins, M.; Lawson, P.; Willems, A.; Cordoba, J.; Fernandez-Garayzabal, J.; Garcia, P.; Farrow, J. The phylogeny of the genus Clostridium: Proposal of five new genera and eleven new species combinations. *Int. J. Syst. Evol. Microbiol.* **1994**, *44*, 812–826. [CrossRef]
53. Nunoura, T.; Hirai, M.; Miyazaki, M.; Kazama, H.; Makita, H.; Hirayama, H.; Takai, K. Isolation and Characterization of a Thermophilic, Obligately Anaerobic and Heterotrophic Marine Chloroflexi Bacterium from a Chloroflexi-dominated Microbial Community Associated with a Japanese Shallow Hydrothermal System, and Proposal for Thermomarinilinea lacunofontalis gen. nov., sp. nov. *Microbes Environ.* **2013**, *28*, 228–235.

54. Yamada, T.; Imachi, H.; Ohashi, A.; Harada, H.; Hanada, S.; Kamagata, Y.; Sekiguchi, Y. Bellilinea caldifistulae gen. nov., sp. nov. and Longilinea arvoryzae gen. nov., sp. nov., strictly anaerobic, filamentous bacteria of the phylum Chloroflexi isolated from methanogenic propionate-degrading consortia. *Int. J. Syst. Evol. Microbiol.* **2007**, *57*, 2299–2306. [CrossRef]
55. Devereux, R.; He, S.; Doyle, C.; Orkland, S.; Stahl, D.; LeGall, J.; Whitman, W. Diversity and origin of Desulfovibrio species: Phylogenetic definition of a family. *J. Bacteriol.* **1990**, *172*, 3609–3619. [CrossRef]
56. Postgate, J.; Campbell, L. Classification of Desulfovibrio species, the nonsporulating sulfate-reducing bacteria. *Bacteriol. Rev.* **1966**, *30*, 732–738.
57. Vita, N.; Valette, O.; Brasseur, G.; Lignon, S.; Denis, Y.; Ansaldi, M.; Pieulle, L. The primary pathway for lactate oxidation in Desulfovibrio vulgaris. *Front. Microbiol.* **2015**, *6*, 606. [CrossRef]
58. Hippe, H.; Vainshtein, M.; Gogotova, G.; Stackebrandt, E. Reclassification of Desulfobacterium macestii as Desulfomicrobium macestii comb. nov. *Int. J. Syst. Evol. Microbiol.* **2003**, *53*, 1127–1130. [CrossRef]
59. Rozanova, E.; Nazina, T.; Galushko, A. Isolation of a new genus of sulfate-reducing bacteria and description of a new species of this genus, Desulfomicrobium apsheronum gen. nov., sp. nov. *Microbiology* **1988**, *57*, 514–520.
60. Reinhold-Hurek, B.; Hurek, T. Reassessment of the taxonomic structure of the diazotrophic genus Azoarcus sensu lato and description of three new genera and new species, Azovibrio restrictus gen. nov., sp. nov., Azospira oryzae gen. nov., sp. nov. and Azonexus fungiphilus gen. nov., sp. nov. *Int. J. Syst. Evol. Microbiol.* **2000**, *50*, 649–660.
61. Chou, J.; Jiang, S.; Cho, J.; Song, J.; Lin, M.; Chen, W. Azonexus hydrophilus sp. nov., a nifH gene-harbouring bacterium isolated from freshwater. *Int. J. Syst. Evol. Microbiol.* **2008**, *58*, 946–951. [CrossRef]
62. Imhoff-Stuckle, D.; Pfennig, N. Isolation and characterization of a nicotinic acid-degrading sulfate-reducing bacterium, Desulfococcus niacini sp. nov. *Arch. Microbiol.* **1983**, *136*, 194–198. [CrossRef]
63. Kuever, J.; Rainey, F.; Widdel, F. Bergey's Manual of Systematics of Archaea and Bacteria. In *Desulfococcus*; John Wiley & Sons, Inc.: Hoboken, NJ, USA, 2015; pp. 1–5.
64. Wolicka, D. *Sulphate-Reducing Bacteria in Biological Treatment Wastewaters*; Nova Science Publishers: New York, NY, USA, 2010.
65. Imhoff, J.; Truper, H.; Pfennig, N. Rearrangement of the species and genera of the phototrophic purple nonsulfur bacteria. *Int. J. Syst. Evol. Microbiol.* **1984**, *34*, 340–343. [CrossRef]
66. Tichi, M.; Tabita, F. Interactive control of Rhodobacter capsulatus redox-balancing systems during phototrophic metabolism. *J. Bacteriol.* **2001**, *183*, 6344–6354. [CrossRef]
67. Dröge, S.; Fröhlich, J.; Radek, R.; König, H. Spirochaeta coccoides sp. nov., a novel coccoid spirochete from the hindgut of the termite Neotermes castaneus. *Appl. Environ. Microbiol.* **2006**, *72*, 392–397. [CrossRef]
68. Leschine, S.; Paster, B.; Canale-Parola, E. Free-living Saccharolytic Spirochetes: The genus Spirochaeta. *Prokaryotes* **2006**, *7*, 195–210.
69. Windsor, H.; Windsor, G.; Noordergraaf, J. The growth and long term survival of Acholeplasma laidlawii in media products used in biopharmaceutical manufacturing. *Biologicals* **2010**, *38*, 204–210. [CrossRef]
70. Wexler, H. Bacteroides: The Good, the Bad, and the Nitty-Gritty. *Clin. Microbiol. Rev.* **2007**, *20*, 593–621. [CrossRef]
71. Martens, E.; Chiang, H.; Gordon, J. Mucosal glycan foraging enhances fitness and transmission of a saccharolytic human gut bacterial symbiont. *Cell Host Microbe* **2008**, *4*, 447–457. [CrossRef]
72. Eberl, L.; Vandamme, P. Members of the genus Burkholderia: Good and bad guys. *F1000Research* **2016**, *2016*, 5. [CrossRef]
73. Hamad, M.; Austin, C.; Stewart, A.; Higgins, M.; Vázquez-Torres, A.; Voskuil, M. Adaptation and Antibiotic Tolerance of Anaerobic Burkholderia pseudomallei. *Antimicrob. Agents Chemother.* **2011**, *55*, 3313–3323. [CrossRef]
74. van Houten, B. Microbial Aspects of Synthesis Gas Fed Bioreactors Treating Sulfate and Metal Rich Wastewaters. Ph.D. Thesis, Wageningen University, Wageningen, The Netherlands, 2006.
75. Elferink, S. Sulfate-Reducing Bacteria in Anaerobic Bioreactors. Ph.D. Thesis, Wageningen Agricultural University, Wageningen, The Netherlands, 1998.
76. Elberson, M.; Sowers, K. Isolation of an aceticlastic strain of Methanosarcina siciliae from marine canyon sediments and emendation of the species description for Methanosarcina siciliae. *Int. J. Syst. Evol. Microbiol.* **1997**, *47*, 1258–1261. [CrossRef]

77. Itoh, T.; Yoshikawa, N.; Takashina, T. Thermogymnomonas acidicola gen. nov., sp. nov., a novel thermoacidophilic, cell wall-less archaeon in the order Thermoplasmatales, isolated from a solfataric soil in Hakone, Japan. *Int. J. Syst. Evol. Microbiol.* **2007**, *57*, 2557–2561. [CrossRef]
78. National Institute of Advanced Industrial Science and Technology. Atlas of Eh-pH Diagrams: Intercomparison of Thermodynamic Databases. 2005. Available online: https://www.nrc.gov/docs/ML1808/ML18089A638.pdf (accessed on 31 August 2019).
79. Meshram, P.; Pandey, B.D.; Mankhand, T.R. Hydrometallurgical processing of spent LIBs in the presence of a reducing agent with emphasis on kinetics of leaching. *Chem. Eng. J.* **2015**, *281*, 418–427. [CrossRef]
80. Falagán, C.; Yusta, I.; Sánchez-España, J.; Johnson, D.B. Biologically-induced precipitation of aluminium in synthetic acid mine water. *Miner. Eng.* **2017**, *106*, 79–85. [CrossRef]
81. Sahinkaya, E.; Gunes, F.; Ucar, D.; Kaksonen, A. Sulfidogenic fluidized bed treatment of real acid mine drainage water. *Bioresour. Technol.* **2011**, *102*, 683–689. [CrossRef]
82. Lewis, A. Review of metal sulphide precipitation. *Hydrometallurgy* **2010**, *104*, 222–234. [CrossRef]